RAD54L regulates replication fork progression and nascent strand degradation in BRCA1/2-deficient cells

Mollie E. Uhrig[1, ^], Neelam Sharma[1], Petey Maxwell[1], Platon Selemenakis[1,$], and Claudia Wiese[1]*

[1]Department of Environmental and Radiological Health Sciences, Colorado State University, Fort Collins, CO 80523, USA

^Graduate Program in Cell and Molecular Biology, Colorado State University, Fort Collins, CO 80523, USA

[$]Present address: Department of Cancer Biology, University of Texas MD Anderson Cancer Center, Houston, TX, USA

* Corresponding author:
Email: claudia.wiese@colostate.edu

Abstract

RAD54L is a DNA motor protein with critical roles in homologous recombination DNA repair (HR). *In vitro*, RAD54L was also shown to catalyze the reversal and restoration of model replication forks. Little, however, is known about the role of RAD54L in regulating the dynamics of DNA replication in cells. Here, we show that RAD54L functions as a fork remodeler and restrains the progression of replication forks in human cells. Analogous to HLTF and FBH1, and consistent with a role in fork reversal, RAD54L catalyzes the slowing of fork progression in response to replication stress. In BRCA1/2-deficient cells, RAD54L activity leads to nascent strand DNA degradation, and loss of RAD54L reduces DNA double-strand break formation. Using a separation-of-function mutation, we show that RAD54L-mediated fork restraint depends on its ability to catalyze branch migration. Our results reveal a new role for RAD54L in regulating the dynamics of replication forks in cells and highlight the impact of RAD54L function on the treatment of patients with BRCA1/2-deficient tumors.

Introduction

Faithful and complete DNA replication is critical for genome stability [1]. Yet, faithful, and complete DNA replication is challenged by genotoxic insult from endogenous or exogenous sources, leading to obstacles in replication fork progression and replication stress. To ameliorate replication stress, cells have acquired several pathways that counteract replication stress and promote the stabilization of stressed replication forks. One such mechanism is through fork reversal [2, 3], a process that involves annealing of the nascent DNA strands. Fork reversal creates a 4-way DNA structure and a double-stranded DNA end, and is associated with a slowdown in fork progression, providing time for lesion bypass and repair [3, 4]. Efficient fork reversal requires the RAD51 recombinase [2, 5-8], the key protein in homologous recombination DNA repair (HR), and several ATP-dependent DNA motor proteins of the SWI2/SNF2 family including SMARCAL1, ZRANB3, and HLTF, and the F-box DNA Helicase 1 (FHB1) [9-13]. Tight regulation of fork reversal is critical for genome stability and dependent on a growing list of fork protection factors [2]. If these factors are dysregulated, fork reversal can lead to unscheduled fork degradation, fueling genome instability [3, 13, 14]. Notably, several key proteins in HR and Fanconi Anemia (FA), such as BRCA1, BRCA2 and FANCD2, have critical roles in protecting reversed forks from degradation [3, 14, 15].

HR, an essential DNA repair pathway, is required for robust DNA replication [16]. HR between sister chromatids ensures that ssDNA gaps are sealed correctly and that collapsed replication forks are rescued through joint molecule formation with the undamaged sister. Joint molecule formation relies on the DNA strand exchange activity of RAD51 and its auxiliary proteins, including RAD54L [17].

RAD54L is a member of the SWI2/SNF2 family of DNA-dependent ATPases [18] and was shown to have multiple roles in HR [19]. During strand invasion, RAD54L utilizes its ATPase activity to convert the synaptic complex into a displacement-loop [20, 21]. RAD54L also removes RAD51 from heteroduplex DNA to allow access of a DNA polymerase for repair synthesis [22, 23]. Independent of its ATPase activity, RAD54L functions at the pre-synaptic stage to stabilize the RAD51 filament [22, 24-26]. *In vitro*, purified RAD54L promotes the branch migration (BM) of Holliday junctions (HJ) and the reversal and restoration of model replication forks [27, 28]. In cells, however, the role of RAD54L in replication fork dynamics has remained enigmatic.

Previous studies carried out in mouse embryonic stem and HeLa cells demonstrated that loss of RAD54L does not lead to the nucleolytic degradation of stalled replication forks [14, 29, 30]. Collectively, the results from these studies suggested that RAD54L plays no major role in the classical FA/BRCA fork protection pathway. However, results obtained in one of our earlier studies [30] suggested that RAD54L may play a role in replication fork restraint. As fork restraint is linked to fork reversal [3, 31], we wondered if RAD54L may function in fork reversal in human cells.

Here, we show that RAD54L restrains replication fork progression in several human cell lines, including cancer and near-normal cells. We show that treatment of cells with PARPi exacerbates accelerated replication fork progression in RAD54L-deficient cells, enhancing the creation of S1 nuclease-sensitive sites. We provide evidence that RAD54L's engagement in fork reversal largely depends on its ability to catalyze BM. Notably, in BRCA1/2-deficient cells, RAD54L activity leads to nascent DNA strand degradation. Collectively, our results show that RAD54L mitigates replication stress, contributes to safeguarding replication fork integrity in human cells by fork reversal, and is a new member in the growing family of proteins engaged in replication fork remodeling.

Materials and Methods

Cell lines, transfections, siRNAs and Western blots

HeLa and MCF7 cells were obtained from ATCC and maintained as recommended. Hs578T cells were a gift from Dr. Joe Gray (OHSU) and maintained as described [32]. hTERT RPE-1 cells were provided by Dr. Tingting Yao (CSU) and maintained as described [33]. HeLa and Hs578T cells that are knockout (KO) for *RAD51AP1* or *RAD54L*, and HeLa *RAD54L KO* cells ectopically expressing RAD54L were maintained as described previously [26, 30, 34]. DLD1 (*BRCA2* KO) cells and DLD1 cells expressing the wild type BRCA2 protein were maintained as described [35].

The negative control siRNA (Ctrl) and siRNAs targeting RAD54L, BRCA1, or BRCA2 were described earlier [26, 36-38] and obtained from IDT (Table S2). For knockdown of HLTF or FBH1, pools of 3 target-specific siRNAs (sc-45943 and sc-90462, respectively) were purchased from Santa Cruz Biotechnology. SiRNA forward transfections with Lipofectamine RNAiMAX (Thermo Fisher Scientific) were performed on two consecutive days. The concentration of siRNAs in transfections was 20 nM each. Cells were treated with drugs at 96 h after the first transfection.

Western blot analyses were performed according to our standard protocols [39]. The following primary antibodies were used: α-RAD51AP1 ([40]; 1:6,000), α-RAD54L (F-11; sc-374598; Santa Cruz Biotechnology; 1:500); α-RAD51 (Ab-1; EMD Millipore; 1:3,000), α-PARP1 (ab6079; Abcam; 1:1,000), α-α-Tubulin (DM1A; Santa Cruz Biotechnology; 1:1,000), α-Histone H3 (ab1791;Abcam; 1:10,000), α-HLTF (E9H5I; 45965; Cell Signaling; 1:6,000) α-FBH1 (sc-81563; 1:100), α-BRCA2 (OP95; EMD Millipore; 1:500), α-BRCA1 (MS110; ab16780; Abcam; 1:50), α-PCNA (sc-25280; Santa Cruz Biotechnology; 1:1,000), α-NUCKS1 ([41]; 1:10,000). HRP-conjugated goat anti-rabbit or goat anti-mouse IgG (Jackson ImmunoResearch; 1:10,000) were used as secondaries. Western blot signals were acquired using a Chemidoc XRS+ gel imaging system and ImageLab software version 5.2.1 (BioRad).

Generation of the MCF7 RAD51AP1 and RAD54L KO cells

To generate MCF7 *RAD51AP1* KO cells, a cocktail of three different CRISPR/Cas9 knockout plasmids (Santa Cruz Biotechnology (sc-408187)) each encoding Cas9 nuclease and one of three different *RAD51AP1*-specific gRNAs targeting exons 2, 3 or 5/6 (Table S3) was used to transfect parental MCF7 cells. To generate MCF7 *RAD54L* KO cells, a combination of two *RAD54L* CRISPR/Cas9-nic KO plasmids each containing one of two different sgRNAs (*i.e.*, sgRNA (54L)-A and sgRNA (54L)-B; Santa Cruz Biotechnology (sc-401750-NIC); Table S3) was used. Disruption of *RAD51AP1* or *RAD54L* was validated by sequence analysis after genomic DNA was isolated from a selection of edited and non-edited clonal isolates using DNeasy Blood & Tissue Kit (Qiagen). *RAD51AP1* and *RAD54L* genomic DNA sequences were amplified by PCR primers flanking the sgRNA target sites (Table S4). PCR products were gel purified, cloned into pCR4-TOPO (Invitrogen) and transformed into TOP10 competent *E. coli*. Plasmid DNA was prepared using ZR Plasmid Miniprep-Classic Kit (Zymo Research) and submitted for sequencing. For each cell line, 15-20 individually cloned amplicons were analyzed by Sanger sequencing.

iPOND assay

The iPOND assay was performed was performed as described [42]. Briefly, 1.5×10^6 HeLa cells were plated in eight 145 mm plates 72 h prior to treatment. Cells were pulse-labeled in 10 μM EdU (Invitrogen) for 20 min and washed twice in PBS. Cells were either fixed immediately or incubated for

2 h in medium containing 3 mM HU. Cells were fixed in 10 ml 1% paraformaldehyde for 10 min prior to quenching the reaction by addition of 1 ml 1.25 M glycine. The cells were washed three times in PBS and harvested using a cell scraper. Cells were spun at 1000×g and 4°C, washed in ice-cold PBS twice, and then flash frozen. To begin protein extraction, cells were permeabilized in 1.5 ml 0.25% Triton X-100/PBS at RT for 30 min. Cell were washed once in 0.5% BSA/PBS and once in PBS before performing the Click-iT reaction with Biotin-Azide (Thermo Fisher Scientific) at RT for 2 h. Then, the cells were pelleted, washed once in 0.5% BSA/PBS and once in PBS, and lysed in lysis buffer (50 mM Tris-HCl [pH 8.0], 1% SDS, and protease/phosphatase inhibitors (Thermo Fisher Scientific)). Cells were sonicated at high setting with 30 s on/off cycles using a Bioruptor UCD-200 (Diagenode). Lysates were cleared by centrifugation at 14000×g. Cleared lysates were diluted with PBS containing protease and phosphatase inhibitors to reduce the final SDS concentration to 0.5% and then incubated with 80 µl equilibrated streptavidin agarose beads (Novex) at 4°C for 16 h. Beads were washed twice with chilled lysis buffer and once with 1M NaCl/PBS before bound proteins were eluted in 80 µl 2×LDS and 95°C for 45 min. Captured proteins were fractionated on NuPAGE gels (Thermo Fisher Scientific) for immunoblot analyses.

Site-directed mutagenesis and lentiviral transduction

Mutations in RAD54L were generated in pENTR1A-RAD54L-HA [30] using the Q5 Site-Directed Mutagenesis Kit (New England Biolabs) (Table S5). pENTR1A constructs were transferred into pLentiCMV/TO DEST#2 [43] using Gateway LR Clonase II (Thermo Fisher Scientific) for the production of lentiviral particles in HEK293FT cells (Thermo Fisher Scientific), as described [43]. Lentivirus was used to transduce HeLa *RAD54L* KO cells in 6 µg/ml polybrene, as described [30, 43].

DNA fiber assay

The DNA fiber assay was performed as described [30]. In the modified fiber assay with S1 nuclease, cells were labeled for 25 min each with 25 µM CldU and 250 µM IdU followed by 10 min in 200 µM thymidine, as described [44]. Cells were harvested in cold PBS, mixed with unlabeled cells (1:1), and centrifuged at 1,500×g and 4°C for 5 min. Cells were resuspended and incubated on ice in hypotonic buffer (10 mM HEPES [pH 7.5], 150 mM NaCl, 0.3 M sucrose, and 0.5% Triton-X-100) for 15 min and then incubated for 10 min at 37°C in S1-nuclease buffer (30 mM sodium acetate [pH 4.6], 10 mM zinc acetate, 5% glycerol, and 50 mM NaCl) with or without 10U/mL S1 nuclease enzyme (Thermo Fisher Scientific). Finally, cells were resuspended in 50 µl lysis buffer (0.5% SDS, 200 mM Tris pH 7.5, 50 mM EDTA). The fibers were spread, imaged, and measured as described [9]. Two slides per sample were prepared for each experimental repeat, and each pair of slides was blinded after immunodetection to avoid bias.

Fiber tract lengths in HeLa and hTERT RPE-1 cell lines were measured to evaluate the consequences of mild replication stress, as described [31]. To do so, cells were pulse labeled with CldU for 20 min followed by IdU containing 25 µM HU for 20 min (HeLa cells) or 30 min (Hela and hTERT RPE-1 cells). Only IdU tracts following a CldU tract were analyzed.

Comet assay

The Comet assay (Trevigen) was performed as recommended by the manufacturer. Cells seeded in 60-mm plates were incubated for 48 hours before 5-hour treatment with 4 mM HU. Cells were harvested in cold PBS and combined with molten low melting (LM) agarose at 1:10. Fifty µL of this mixture were spread on comet slides and incubated for 30 min at 4°C in the dark. The slides were then incubated

overnight at 4°C in lysis buffer. Following a 30 min incubation in neutral comet electrophoresis buffer (10 mM Tris base, 250 mM sodium acetate) at 4°C, electrophoresis was performed at 25V and 4°C for 30 min in the neutral electrophoresis buffer. The slides were then incubated in DNA precipitation solution (7.5 M NH_4Ac and 95% ethanol) for 30 min followed by 30 min incubation in 70% ethanol. Slides were dried at 37°C for 1 hour and stained with 0.3× SYBR Gold (Thermo Fisher). Images were acquired on a Zeiss Axio-Imager.Z2 microscope equipped with Zen Blue software (Carl Zeiss Microscopy) using a 20× objective, and 100 comets were measured per condition. The lengths of the comet tails were measured using ImageJ software (https://imagej.net).

Statistics and reproducibility

GraphPad Prism 9 software was used to perform statistical analyses on data obtained from 3 independent experiments. To assess statistical significance ANOVA tests were performed as indicated, and $P \leq 0.05$ was considered significant.

Results

RAD54L is bound to stalled DNA replication forks

To begin exploring the involvement of RAD54L in replication fork progression in human cells, we applied the isolation of proteins on nascent DNA (iPOND) assay [42]. In accordance with results from others [29], we show that RAD54L is enriched at replication forks upon a 2h-treatment of HeLa cells with 3 mM hydroxyurea (HU) (Fig. 1A, B). Enrichment of RAD54L mirrored that of its binding partners RAD51 and NUCKS1. In contrast, enrichment of PCNA was downregulated after HU, as expected. These results demonstrate RAD54L recruitment to stalled replication forks.

RAD54L restrains replication fork progression in unperturbed cells

Previously, we generated HeLa RAD54L KO cells and RAD54L KO cells ectopically expressing HA-tagged RAD54L, which fully rescues the sensitivity of RAD54L KO cells to mitomycin C (MMC) or olaparib [30]. Using the single molecule DNA fiber assay, we noticed in HeLa cells that the RAD54L KO had longer replication tracts than the control [30]. These results were independently replicated here (Fig. 1C-E; Fig. S1A). We also generated RAD54L KOs in Hs578T [30] and MCF cells (Fig. 1C; Table S1), and both Hs578T RAD54L KO and MCF7 RAD54L KO cells show longer replication tracts than parental cells (Fig. 1E; Fig. S1B, C). Moreover, as in HeLa cells [30], tracts in the RAD54L KOs were significantly longer than those in Hs578T or MCF7 cells deficient in RAD51AP1 (Fig. 1E; Fig. S1B, C). As RAD54L, RAD51AP1 is a RAD51-associated protein that promotes RAD51 recombinase activity [45, 46]. These results show that unperturbed DNA replication proceeds faster in the absence of RAD54L and that this is not cell-type specific.

RAD54L is dispensable for the recovery of cells from stalled replication

To understand the fate of stalled replication forks, we treated the Hs578T cell derivatives with 4 mM HU for 5 h, which blocks DNA synthesis and stalls replication fork movement [13]. Using the DNA fiber assay, we then monitored the recovery of cells from stalled replication (Fig. 2A). We determined the ability of Hs578T cells and derivatives to restart DNA replication by measuring the lengths of IdU tracts proceeded by a CldU tract. The results show that RAD54L-deficient Hs578T cells recover as fast as wild type cells from stalled DNA replication (Fig. 2B, right panel; Fig. S2A). In contrast, RAD51AP1-deficient Hs578T cells are significantly impaired in fork restart. These results mirror our published

results in HeLa cells [30] and demonstrate that RAD54L is dispensable for the recovery from stalled DNA replication in human cells.

RAD54L slows fork progression upon nucleotide depletion

In response to replication stress, replication forks reverse into four-way junctions through annealing of the nascent DNA strands [2, 8]. Reversed forks must be protected from nucleolytic attack to prevent fork attrition [9, 12, 14, 47, 48]. To assess if RAD54L in Hs578T cells functions in the protection of replication forks from unprogrammed nuclease degradation, CldU tracts in cells exposed to HU were measured. The results show that that CldU tracts in Hs578T RAD54L KO cells are not shorter than in parental cells (Fig. 2C, right panel; Fig. S2A). Hence, RAD54L appears to play no major role in protecting reversed forks from nuclease attrition in cells with otherwise unaltered fork protection pathways. These results are in accord with earlier studies using different cell types [14, 29, 30].

Previous studies have shown that a defect in replication fork restraint is linked to compromised fork reversal [2, 31, 49, 50]. Previous studies have also shown that RAD54L has BM activity and can reverse model replication forks *in vitro* [27, 28, 51]. Prompted by our findings that identified a defect in replication fork restraint in RAD54L-deficient cells (Fig. 1E; Fig. 2B), we monitored fork progression in HeLa cell derivatives under a low concentration of HU (25 μM) given within the IdU pulse (Fig. 2D). In these experiments, we measured the lengths of IdU tracts following a CldU tract. Under exposure to low concentrations of HU, replication tracts in two independently isolated RAD54L KO lines [30] were significantly longer than those in parental or rescued cells (Fig. 2E; Fig. S2B). These results show that in response to HU, which induces fork reversal [47], accelerated fork progression is a consequence of RAD54L deficiency. These results suggest that RAD54L catalyzes fork reversal *in vivo*.

Next, we used the same DNA fiber assay protocol (Fig. 2D) to compare the consequences of RAD54L deficiency to loss of HLTF or FBH1, two established fork remodeling proteins [13, 31, 50, 52, 53]. To do so, we depleted RAD54L, HLTF, or FBH1 in HeLa cells and measured IdU tract lengths in the presence of 25 μM HU. As observed previously in different cell types [13, 31], loss of HLTF or FBH1 expression led to significantly longer replication tracts than in control cells (Fig. 2F, G; Fig. S2C). Of note, after depletion of RAD54L IdU tracts were also significantly longer than in control cells (Fig. 2F, G; Fig. S2C).

Last, we tested if loss of RAD54L expression would lead to a defect in fork restraint in non-cancerous hTERT RPE-1 cells. We depleted RAD54L in hTERT RPE-1 cells and measured IdU tract lengths (Fig. 2H), as described above. Compared to control cells transfected with a non-depleting Ctrl siRNA, IdU tracts were significantly longer in RAD54L-deficient hTERT RPE-1 cells (Fig. 2J, I; Fig. S2D). Collectively, our results show that RAD54L's ability to restrain fork progression is not confined to cancer cell lines and occurs in both unperturbed cells (Fig. 1E) and upon exposure of cells to mild replications stress (Fig. 2E, F, I).

Accelerated fork progression in RAD54L-deficient cells is associated with ssDNA gap formation

Treatment of cells with a PARP1 inhibitor (PARPi) leads to accelerated fork progression, impediments in nascent DNA strand maturation, and fork collapse [54-57]. RAD54L-deficient cells are sensitive to the PARPi Olaparib [30, 33], and treatment of RAD54L KO cells with Olaparib exacerbates fork progression (Fig. 3A, B; Fig. S3A; [30]). Expression of ectopic RAD54L in RAD54L KO cells reverses accelerated fork progression, as expected (Fig. 3B; Fig. S3A).

To test for the presence of ssDNA formed at replication gaps, we incubated control cells and cells treated with Olaparib with and without S1 nuclease (Fig. 3C). S1 nuclease cleaves replication intermediates that

contain ssDNA [58]. In these experiments, we assessed the derivatives of both HeLa and Hs578T cells and found that S1 treatment more prominently shortened replication tracts in cells deficient in RAD54L (Fig. 3D, F; Fig. S3A, B). Treatment of cells with Olaparib exacerbated replication tract shortening in RAD54L KO cells (Fig. 3E, G; Fig. S3A, B). These results show that replication proceeds with the production of ssDNA gaps in the absence of RAD54L.

Loss of RAD54L restores fork stability in BRCA1/2-deficient cells

The activities of SMARCAL1, ZRANB3, and HTLF lead to the degradation of nascent strand DNA in BRCA1/2-deficient cells upon treatment with HU [8, 9]. Given our results that suggest that RAD54L may function similarly to these established fork remodelers, we tested if RAD54L loss may prevent nascent strand DNA degradation in BRCA1/2-deficient cells (Fig. 4A). We depleted BRCA2 in HeLa, RAD54L KO, and RAD54L-rescued cell lines (Fig. 4B) and measured fork degradation in response to a 5 h treatment with 4 mM HU. As expected, BRCA2 knockdown in HeLa and RAD54L KO+RAD54L cells led to significantly reduced IdU/CldU tract ratios (Fig. 4C; Fig. S4E). In contrast, forks in RAD54L KO cells with BRCA2 knockdown withstood fork attrition (Fig. 4C; Fig. S4E). Similarly, IdU/CldU tract ratios in HeLa cells with BRCA1 knockdown were reduced, while no such effect was observed in RAD54L KO cells with BRCA1 knockdown (Fig. S4A-D). These results show that RAD54L loss in BRCA-deficient HeLa cells prevents nascent strand DNA degradation in response to HU.

Next, we used DLD1 (BRCA2 KO) cells and a DLD1 cell line stably expressing the wild type BRCA2 protein [35] and depleted RAD54L in these two cell lines. As expected and shown previously [35], IdU/CldU tract length ratios were significantly reduced in DLD1 cells after treatment with HU (Fig. 4E; Fig. S4F). In contrast, knockdown of RAD54L in HU-treated DLD1 cells gave rise to IdU/CldU tract ratios with a distribution not significantly different to that from DLD1+BRCA2 cells (Fig. 4E; Fig. S4F). These results show that RAD54L loss in BRCA2-deficient DLD1 cells prevents nascent strand DNA degradation in response to HU.

To assess the impact of RAD54L deficiency on DSB formation in DLD1 cells, we subjected DLD1 and DLD1+BRCA2 cells (transfected with Ctrl or RAD54L siRNA) upon exposure to HU to DSB detection by neutral comet assay. Consistent with our results for fork degradation (Fig. 4E), depletion of RAD54L in DLD1+BRCA2 cells had no significant impact on DSB formation (Fig. 4F; Fig. S4G). In contrast, depletion of RAD54L in DLD1 (BRCA2 KO) cells led to significantly reduced DSB formation (Fig. 4F; Fig. S4G). These results show that loss of RAD54L limits HU-induced DNA damage in BRCA2-deficient DLD1 cells.

RAD54L's branch migration attribute contributes to its engagement in fork reversal

Fork reversal is a two-step process, in which fork regression is followed by BM to drive extensive reversal [59]. RAD54L catalyzes BM, and its N-terminal domain is essential for this activity [28]. As N-terminal mutations in RAD54L that selectively inhibit its BM have been described [28], we asked if RAD54L BM mutants would show defects in fork restraint. To this end, we expressed mutant RAD54L-S49E (deficient in oligomerization [28]) and RAD54L-4A/S49E (deficient in binding to HJ-like DNA structures and oligomerization [28]) in RAD54L KO cells (Fig. 5A, B). To assess defects in fork restraint, we chose the protocol as depicted in Fig. 5C and compared the response of RAD54L KO cells expressing mutant RAD54L to that of RAD54L KO cells with and without wild type RAD54L. As shown above (Fig. 2E, F) and reproduced here independently, RAD54L KO cells exhibit a significant defect in fork restraint (Fig. 5C; Fig. S5). Fork restraint also is impaired in RAD54L-S49E and RAD54L-4A/S49E cells with a significantly more pronounced defect in RAD54L-4A/S49E expressing cells compared to

RAD54L-S49E expressing cells (Fig. 5C; Fig. S5). These results show that RAD54L BM activity is critical for fork restraint.

Discussion

Our work establishes that RAD54L catalyzes the slowing of replication fork progression in human cells. Moreover, we provide evidence that RAD54L's ability to catalyze BM is critical for fork restraint. Our observations corroborate biochemical evidence [27] and are in strong support of RAD54L catalyzing replication fork reversal in human cells (Fig. 5E). Accordingly, we show that RAD54L activity leads to the degradation of stressed replication forks in BRCA1/2-deficient cells.

Purified RAD54L uses its BM activity to catalyze both the regression and restoration of model replication forks [27]. In the presence of RAD51 (as would be the situation in cells), however, the reaction was shifted toward the accumulation of the chicken foot structure [27]. Our results are in line with this biochemical study and now have added one more attribute to the multi-functional RAD54L protein- limiting replication stress through fork restraint in human cells.

Genetic and biochemical studies have delineated that fork reversal in human cells is catalyzed by the FBH1 helicase or three DNA translocases of the SNF2 family: SMARCAL1, ZRANB3 and HLTF [13, 60]. The SNF2 protein family structurally contains a SWI/SNF (switch/sucrose non-fermenting) translocase domain with a bi-lobed RecA-type ATPase and includes the RAD54-like proteins and RAD54L [18]. RAD54L is known as an important HR factor, promoting RAD51-mediated strand invasion, homology search, nucleosome remodeling, and removal of RAD51 from dsDNA [21, 61-64]. One step in the HR reaction is the formation of a HJ that can branch migrate along DNA, affecting the length of heteroduplex DNA. Purified RAD54L binds to HJ-like DNA substrates with high specificity and promotes their bidirectional BM in an ATPase-dependent manner [65, 66]. Yet, we predict that the defect in fork restraint of the ATPase-deficient RAD54L-K189R would be comparable to that of cells lacking RAD54L.

In human cells, the inhibition of fork reversal leads to unrestrained fork progression [49, 50, 67, 68]. RAD54L KO cells and RAD54L KO cells expressing established RAD54L BM mutants [28] have significant defects in fork restraint, suggesting that RAD54L BM activity plays an important role in RAD54L's ability to slow replication forks. RAD54L BM mutants, however, are not as defective in fork restraint as RAD54L KO cells, which may be related to additional attributes of RAD54L contributing to fork restraint [8]. Of note, RAD54L BM mutants retain translocase, stimulation of RAD51-mediated strand exchange, and ATPase activities [28]. All of which may additionally contribute to fork restraint, as shown, for example, for the ATPase motifs in SMARCAL1, ZRANB3, and HLTF [9, 69].

Reminiscent of proteins with established functions in catalyzing fork reversal [2, 9, 10, 59], loss of RAD54L leads to reduced HU-induced DNA damage in BRCA1/2-deficient cells. As such, diminished or compromised RAD54L may affect the response of BRCA1/2-deficient tumors to replication stress-inducing chemotherapy. Therefore, the results presented here not only contribute to a better understanding of the activities of the RAD54L DNA motor protein but also may help guide further optimized treatment strategies of patients with BRCA1/2-deficient tumors.

Funding

This work was supported by National Institutes of Health Grant R01GM144579.

CRediT authorship contribution statement

Mollie E. Uhrig: Investigation, methodology, validation, formal analysis. **Neelam Sharma:** Investigation, methodology, validation. **Petey Maxwell:** Validation. **Platon Selemenakis:** Investigation, critical reagents. **Claudia Wiese:** Conceptualization, formal analysis, writing of the manuscript, funding acquisition.

Conflict of interest statement

The authors declare that there is no conflict of interest.

Appendix A. Supplementary data

Supplementary material related to this manuscript is available.

Figures and legends

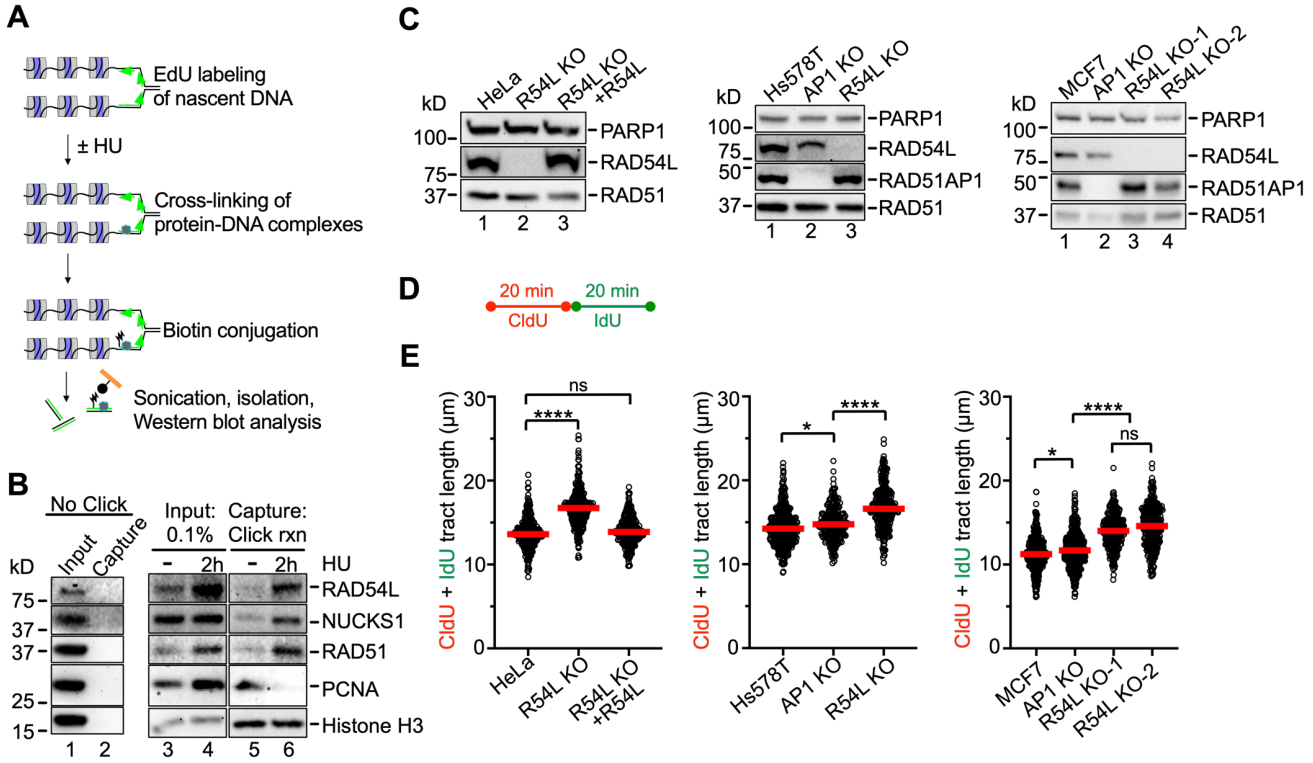

Fig. 1 RAD54L is enriched at stalled replication forks and restrains replication fork progression. (**A**) Schematic illustration of the iPOND assay. (**B**) Western blots of the input and iPOND samples probed for proteins, as indicated. NUCKS1 is a RAD54L interacting protein [26]. Click rxn, Click reaction; the no Click condition represents cells pulsed with EdU and processed without biotin-azide in the Click reaction step. (**C**) Western blots of HeLa, *RAD54L* KO, and *RAD54L* KO cells ectopically expressing RAD54L-HA, as described earlier [30]. (**D**) Schematic of the protocol for the DNA fiber assay to determine replication tract lengths. (**E**) Dot plot with medians of CldU+IdU tract lengths in

parental cells and RAD54L (R54L) KOs in Hela, Hs578T, and MCF7 cells. RAD51AP1 KOs (AP1) and R54L KOs ectopically expressing R54L (R54L KO+R54L; [30]) are show for comparison purposes (n=3; at least 100 fiber tracts/experiment analyzed). Fiber tract lengths were analyzed by Kruskal-Wallis test followed by Dunn's multiple comparisons test (ns, not significant; *, p<0.05; ****, p<0.0001).

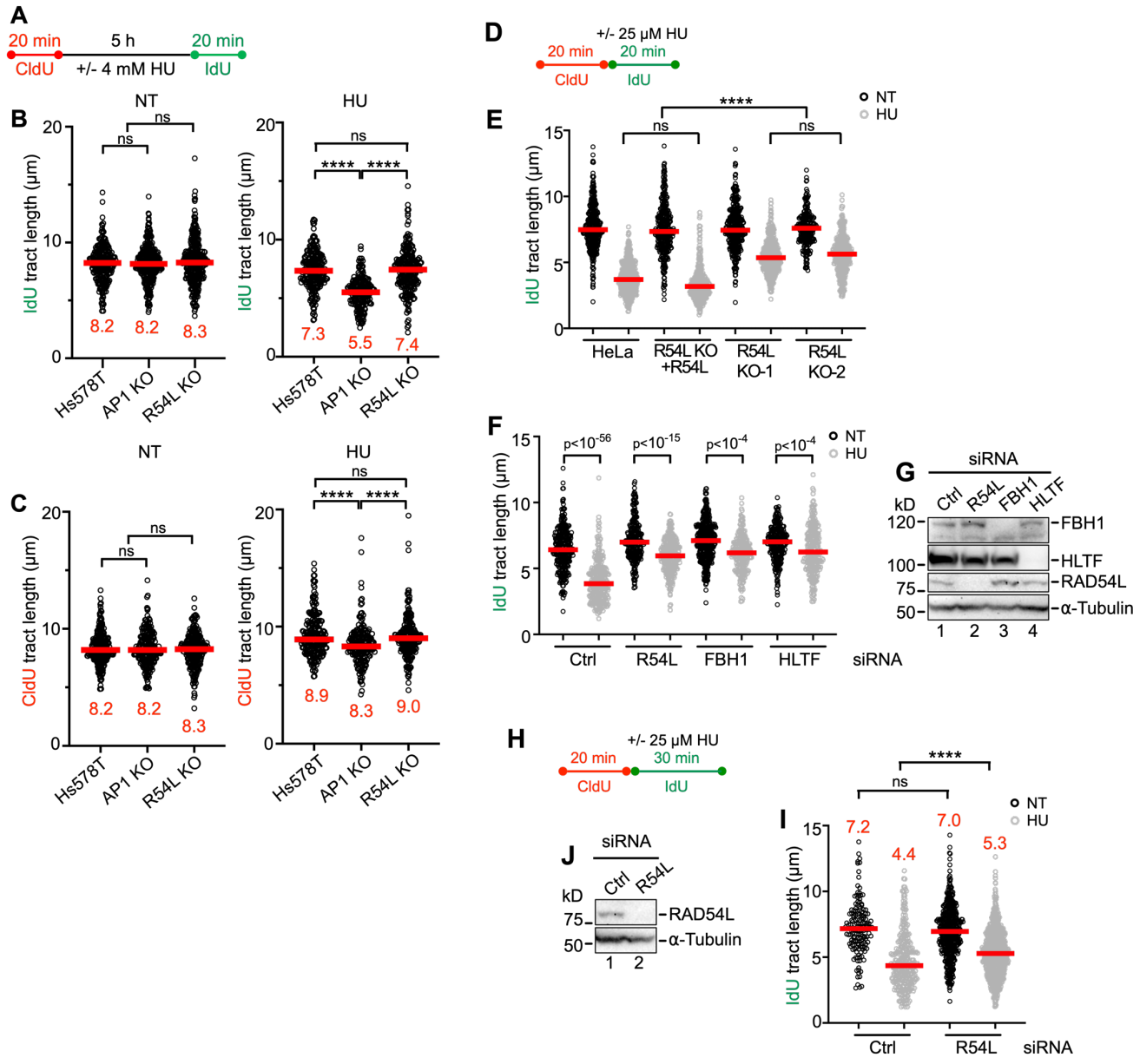

Fig. 2 RAD54L loss does not affect replication restart after HU and leads to longer replication tracts during mild replication stress. (**A**) Schematic of the DNA fiber assay protocol used to assess replication restart. (**B**) Dot plot with medians of IdU tract lengths in untreated (NT) or HU treated Hs578T and RAD51AP1 (AP1) or RAD54L (R54L) KO cells. (**C**) Dot plot with medians of CldU tract lengths in untreated (NT) or HU treated Hs578T and RAD51AP1 (AP1) or RAD54L (R54L) KO cells. (n=3; at least 100 fiber tracts/experiment analyzed). (**D**) Schematic of the DNA fiber assay protocol used to evaluate replication progression during mild replication stress in HeLa cells and derivatives. (**E**) Dot

plot with medians of IdU tract lengths in HeLa control cells, R54L KO+R54L, and two independently isolated R54L KO cell lines treated with or without 25 μM HU during the IdU pulse (n=3; at least 100 fiber tracts/experiment analyzed). (**F**) Dot plot with medians of IdU tract lengths in HeLa cells transfected with control (Ctrl), R54L, FBH1, or HLTF siRNA and treated with or without 25 μM HU during the IdU pulse (n=3; at least 100 fiber tracts/experiment analyzed). (**G**) Representative Western blots to show extent of protein knockdown for the experiments shown in F. Loading control: α-Tubulin. (**H**) Schematic of the DNA fiber assay protocol used to evaluate replication progression during mild replication stress in hTERT RPE-1 cells. (**I**) Dot plot with medians of IdU tract lengths in hTERT RPE-1 cells transfected with control (Ctrl) or R54L siRNA and treated with or without 25 μM HU during the IdU pulse (n=3; at least 100 fiber tracts/experiment analyzed). (**J**) Representative Western blots to show extent of protein knockdown for the experiments shown in I. Loading control: α-Tubulin. Fiber tract lengths were analyzed by Kruskal-Wallis test followed by Dunn's multiple comparisons test (ns, not significant; ****, p<0.0001, or as indicated).

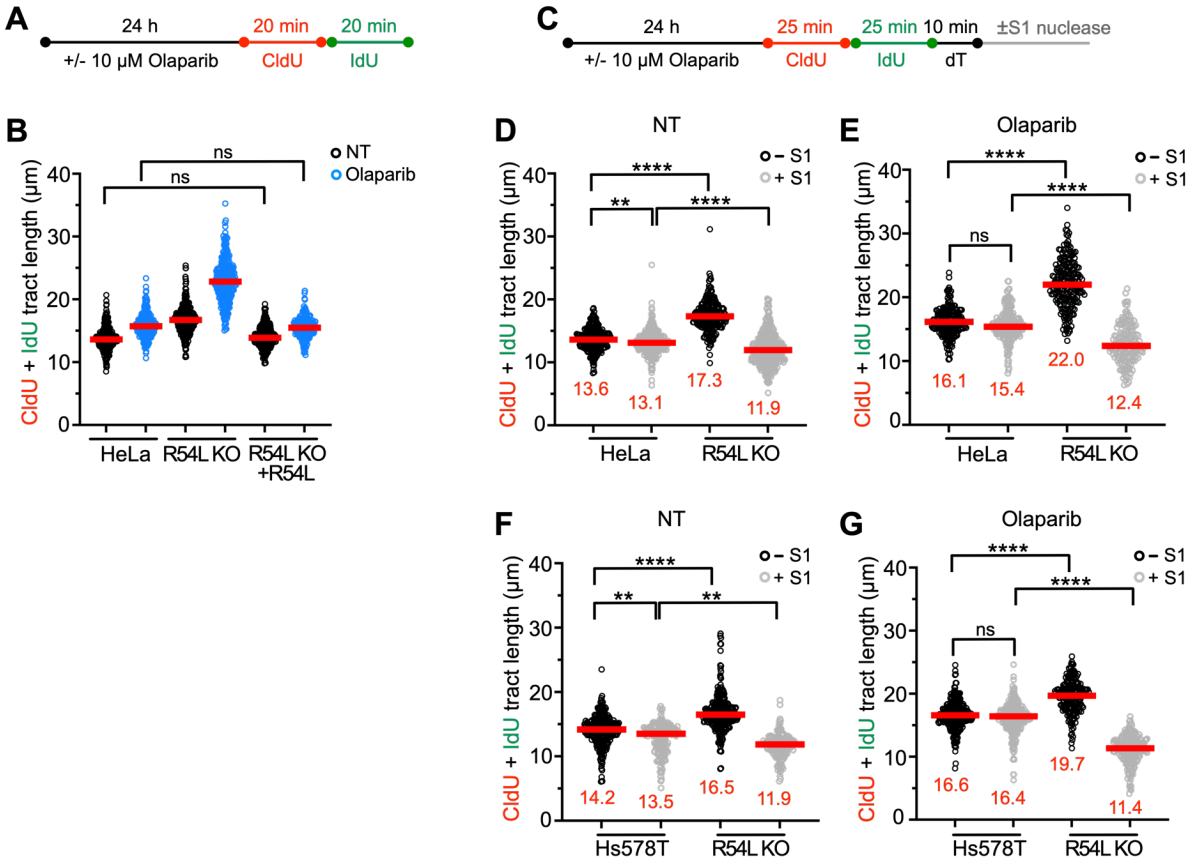

Fig. 3 Loss of RAD54L accelerates replication fork progression and ssDNA gap formation. (**A**) Schematic of the DNA fiber assay protocol to assess fork progression with and without Olaparib. (**B**) Dot plot with medians of CldU+IdU fiber tract lengths in HeLa, R54L KO, and R54L KO+R54L cells with or without Olaparib (n=3; at least 100 fiber tracts/experiment analyzed). (**C**) Schematic of the modified DNA fiber assay protocol with S1 nuclease in unperturbed and Olaparib treated cells. (**D**) Dot plot with medians of CldU+IdU fiber tract lengths in untreated (NT) HeLa and R54L KO cells with or without S1 nuclease (n=3; at least 100 fiber tracts/experiment analyzed). (**E**) Dot plot with medians of

CldU+IdU fiber tract lengths in HeLa and R54L KO cells treated with Olaparib and with or without S1 nuclease (n=3; at least 100 fiber tracts/experiment analyzed). (**F**) Dot plot with medians of CldU+IdU fiber tract lengths in untreated (NT) Hs578T and R54L KO cells with or without S1 nuclease (n=3; at least 100 fiber tracts/experiment analyzed). (**G**) Dot plot with medians of CldU+IdU fiber tract lengths in Hs578T and R54L KO cells treated with Olaparib and with or without S1 nuclease (n=3; at least 100 fiber tracts/experiment analyzed). Fiber tract lengths were analyzed by Kruskal-Wallis test followed by Dunn's multiple comparisons test (ns, not significant; (**, p<0.01; ****, p<0.0001).

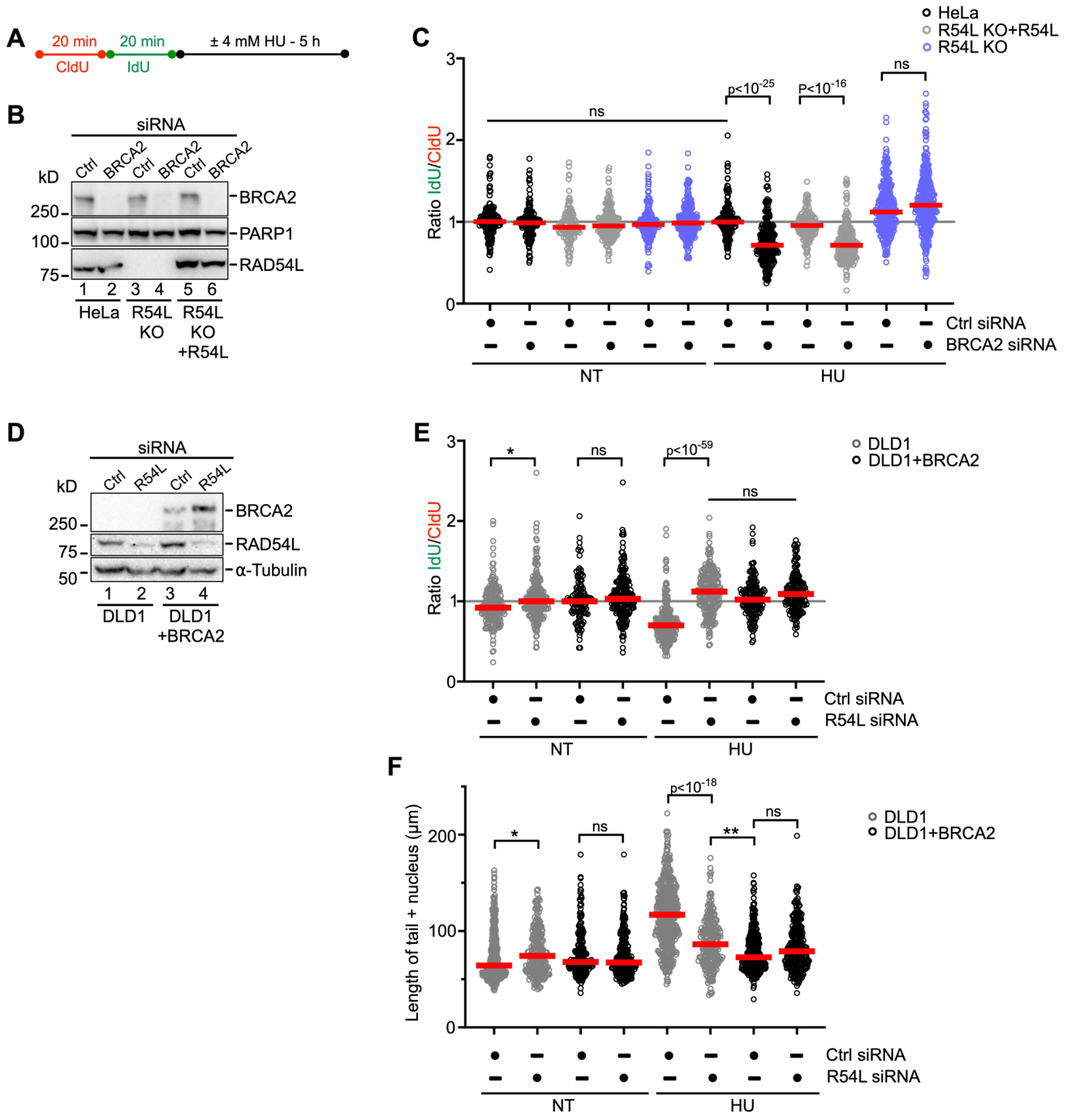

Fig. 4 Loss RAD54L prevents fork degradation and DSB formation in BRCA2-deficient cells. (**A**) Schematic of the DNA fiber assay protocol to assess fork degradation after HU. (**B**) Representative Western blots to show extent of BRCA2 knockdown in HeLa cells and derivatives for the experiments shown in C. Loading control: PARP1. (**C**) Dot plot with medians of IdU/CldU tract length ratios in HeLa, R54L KO, and R54L KO+R54L cells transfected with Ctrl or BRCA2 siRNA and treated with or without HU (n=3; at least 100 fiber tracts/experiment analyzed). (**D**) Representative Western blots to show extent of RAD54L knockdown in DLD1 cells (BRCA2 KO) and DLD1 cells expressing BRCA2 [35] for the experiments shown in E and F. and derivatives for the experiments shown in C. Loading control: α-Tubulin. (**E**) Dot plot with medians of IdU/CldU tract length ratios in DLD1 and DLD1+BRCA2 cells transfected with Ctrl or RAD54L siRNA and treated with or without HU (n=3; at least 100 fiber tracts/experiment analyzed). (**F**) Dot plot with medians after neutral Comet assay in DLD1 and DLD1+BRCA2 cells transfected with Ctrl or RAD54L siRNA and treated with or without HU (n=3; at least 100 Comet tails/experiment analyzed). IdU/CldU ratios and length of Comet signals were analyzed by Kruskal-Wallis test followed by Dunn's multiple comparisons test (ns, not significant; *, p<0.05; **, p<0.01, or as indicated).

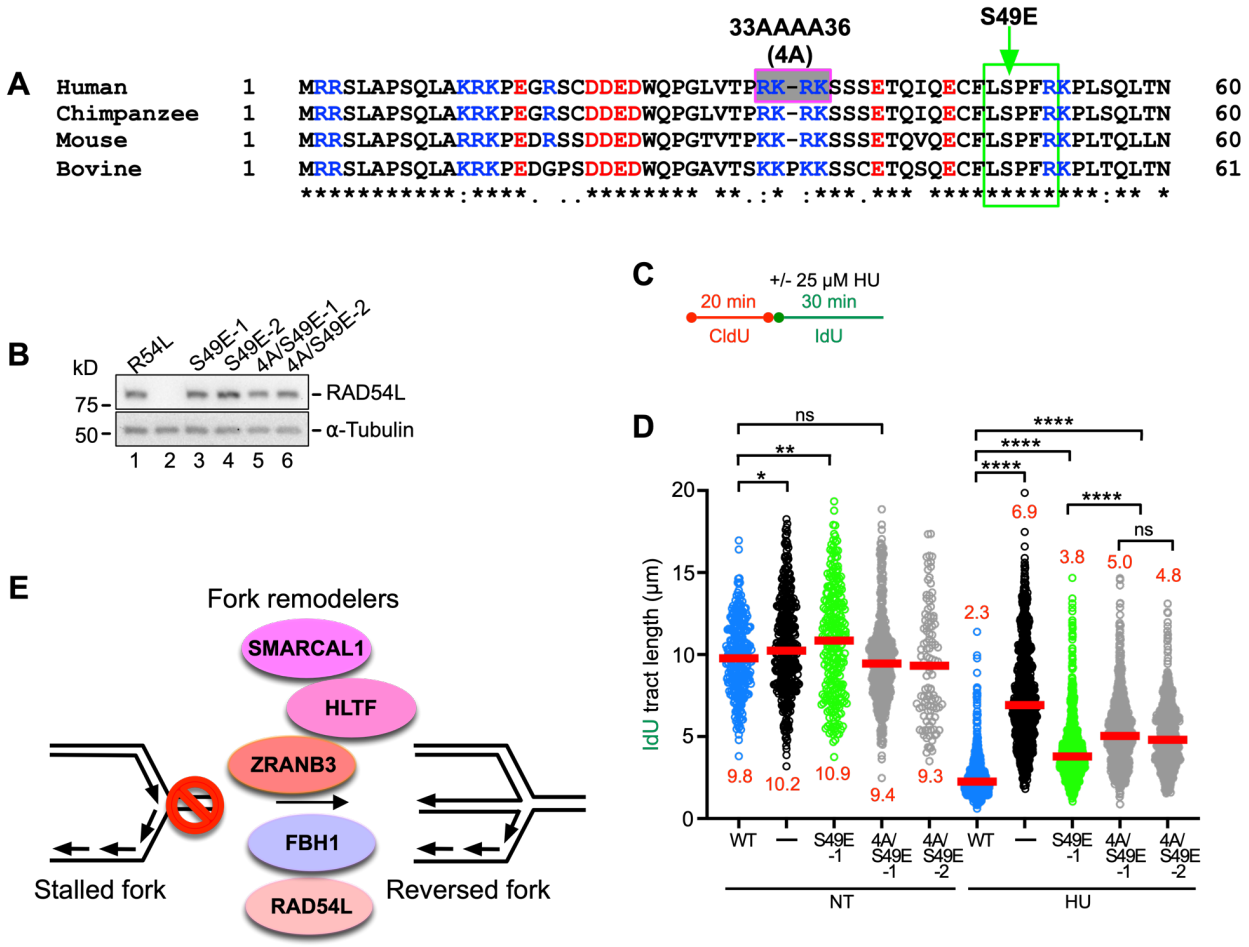

Fig. 5 RAD54L's branch migration activity contributes to its ability to restrain replication fork progression. (**A**) ClustalW sequence alignment of the N-terminal domains of RAD54L from human (Homo sapiens), chimpanzee (Pan troglodytes), mouse (Mus musculus), and bovine (Bos taurus). Basic residues are shown in blue, and acidic residues are shown in red. The pink box indicates basic residues

mutated to alanines, and the green box indicates CDK2 phosphorylation consensus sequence and mutated serine to glutamate, as previously described [28]. (**B**) Representative Western blots to show expression of wild type RAD54L (lane 1) and RAD54L mutants (lanes 3-6) in HeLa RAD54L KO cells. RAD54L-S49E expressing lines are clonal isolates resistant to puromycin; RAD54L-4A/S49E expressing cells are puromycin-resistant cell populations. Loading control: α-Tubulin. (**C**) Schematic of the DNA fiber assay protocol used in D. (**D**) Dot plot with medians of IdU tract lengths in HeLa RAD54L KO cells expressing wild type RAD54L (WT) or RAD54L mutants (S49E and 4A/S49E) treated with or without 25 μM HU during the IdU pulse (n=3; at least 100 fiber tracts/experiment analyzed). Fiber tract lengths were analyzed by Kruskal-Wallis test followed by Dunn's multiple comparisons test (ns, not significant; (∗, $p<0.05$; ∗∗, $p<0.01$; ∗∗∗∗, $p<0.0001$). (**E**) Model to show that RAD54L contributes to fork reversal in human cells.

References

1. Saxena, S. and L. Zou, *Hallmarks of DNA replication stress.* Mol Cell, 2022. **82**(12): p. 2298-2314.
2. Zellweger, R., et al., *Rad51-mediated replication fork reversal is a global response to genotoxic treatments in human cells.* J Cell Biol, 2015. **208**(5): p. 563-79.
3. Thakar, T. and G.L. Moldovan, *The emerging determinants of replication fork stability.* Nucleic Acids Res, 2021. **49**(13): p. 7224-7238.
4. Tye, S., G.E. Ronson, and J.R. Morris, *A fork in the road: Where homologous recombination and stalled replication fork protection part ways.* Semin Cell Dev Biol, 2020.
5. Mason, J.M., et al., *Non-enzymatic roles of human RAD51 at stalled replication forks.* Nat Commun, 2019. **10**(1): p. 4410.
6. Hashimoto, Y., et al., *Rad51 protects nascent DNA from Mre11-dependent degradation and promotes continuous DNA synthesis.* Nat Struct Mol Biol, 2010. **17**(11): p. 1305-11.
7. Kavlashvili, T., et al., *Replication fork uncoupling causes nascent strand degradation and fork reversal.* Nat Struct Mol Biol, 2023. **30**(1): p. 115-124.
8. Liu, W., et al., *RAD51 bypasses the CMG helicase to promote replication fork reversal.* Science, 2023. **380**(6643): p. 382-387.
9. Taglialatela, A., et al., *Restoration of Replication Fork Stability in BRCA1- and BRCA2-Deficient Cells by Inactivation of SNF2-Family Fork Remodelers.* Mol Cell, 2017. **68**(2): p. 414-430 e8.
10. Kolinjivadi, A.M., et al., *Smarcal1-Mediated Fork Reversal Triggers Mre11-Dependent Degradation of Nascent DNA in the Absence of Brca2 and Stable Rad51 Nucleofilaments.* Mol Cell, 2017. **67**(5): p. 867-881 e7.
11. Mijic, S., et al., *Replication fork reversal triggers fork degradation in BRCA2-defective cells.* Nat Commun, 2017. **8**(1): p. 859.
12. Lemacon, D., et al., *MRE11 and EXO1 nucleases degrade reversed forks and elicit MUS81-dependent fork rescue in BRCA2-deficient cells.* Nat Commun, 2017. **8**(1): p. 860.
13. Liu, W., et al., *Two replication fork remodeling pathways generate nuclease substrates for distinct fork protection factors.* Sci Adv, 2020. **6**(46).
14. Schlacher, K., et al., *Double-strand break repair-independent role for BRCA2 in blocking stalled replication fork degradation by MRE11.* Cell, 2011. **145**(4): p. 529-42.
15. Schlacher, K., H. Wu, and M. Jasin, *A distinct replication fork protection pathway connects Fanconi anemia tumor suppressors to RAD51-BRCA1/2.* Cancer Cell, 2012. **22**(1): p. 106-16.

16. Costes, A. and S.A. Lambert, *Homologous recombination as a replication fork escort: fork-protection and recovery.* Biomolecules, 2012. **3**(1): p. 39-71.
17. Zhao, W., et al., *The BRCA Tumor Suppressor Network in Chromosome Damage Repair by Homologous Recombination.* Annu Rev Biochem, 2019. **88**: p. 221-245.
18. Flaus, A., et al., *Identification of multiple distinct Snf2 subfamilies with conserved structural motifs.* Nucleic Acids Res, 2006. **34**(10): p. 2887-905.
19. Ceballos, S.J. and W.D. Heyer, *Functions of the Snf2/Swi2 family Rad54 motor protein in homologous recombination.* Biochim Biophys Acta, 2011. **1809**(9): p. 509-23.
20. Sigurdsson, S., et al., *Homologous DNA pairing by human recombination factors Rad51 and Rad54.* J Biol Chem, 2002. **277**(45): p. 42790-4.
21. Crickard, J.B., et al., *Rad54 Drives ATP Hydrolysis-Dependent DNA Sequence Alignment during Homologous Recombination.* Cell, 2020. **181**(6): p. 1380-1394 e18.
22. Agarwal, S., et al., *ATP-dependent and independent functions of Rad54 in genome maintenance.* J Cell Biol, 2011. **192**(5): p. 735-50.
23. Wright, W.D. and W.D. Heyer, *Rad54 functions as a heteroduplex DNA pump modulated by its DNA substrates and Rad51 during D loop formation.* Mol Cell, 2014. **53**(3): p. 420-32.
24. Mazin, A.V., A.A. Alexeev, and S.C. Kowalczykowski, *A novel function of Rad54 protein. Stabilization of the Rad51 nucleoprotein filament.* J Biol Chem, 2003. **278**(16): p. 14029-36.
25. Sanchez, H., et al., *Combined optical and topographic imaging reveals different arrangements of human RAD54 with presynaptic and postsynaptic RAD51-DNA filaments.* Proc Natl Acad Sci U S A, 2013. **110**(28): p. 11385-90.
26. Maranon, D.G., et al., *NUCKS1 promotes RAD54 activity in homologous recombination DNA repair.* J Cell Biol, 2020. **219**(10).
27. Bugreev, D.V., M.J. Rossi, and A.V. Mazin, *Cooperation of RAD51 and RAD54 in regression of a model replication fork.* Nucleic Acids Res, 2011. **39**(6): p. 2153-64.
28. Goyal, N., et al., *RAD54 N-terminal domain is a DNA sensor that couples ATP hydrolysis with branch migration of Holliday junctions.* Nat Commun, 2018. **9**(1): p. 34.
29. Spies, J., et al., *Nek1 Regulates Rad54 to Orchestrate Homologous Recombination and Replication Fork Stability.* Mol Cell, 2016. **62**(6): p. 903-917.
30. Selemenakis, P., et al., *RAD51AP1 and RAD54L Can Underpin Two Distinct RAD51-Dependent Routes of DNA Damage Repair via Homologous Recombination.* Front Cell Dev Biol, 2022. **10**: p. 866601.
31. Bai, G., et al., *HLTF Promotes Fork Reversal, Limiting Replication Stress Resistance and Preventing Multiple Mechanisms of Unrestrained DNA Synthesis.* Mol Cell, 2020. **78**(6): p. 1237-1251 e7.
32. Colston, K.W., et al., *Growth inhibition of both MCF-7 and Hs578T human breast cancer cell lines by vitamin D analogues is associated with increased expression of insulin-like growth factor binding protein-3.* J Mol Endocrinol, 1998. **20**(1): p. 157-62.
33. Olivieri, M., et al., *A Genetic Map of the Response to DNA Damage in Human Cells.* Cell, 2020. **182**(2): p. 481-496 e21.
34. Liang, F., et al., *DNA requirement in FANCD2 deubiquitination by USP1-UAF1-RAD51AP1 in the Fanconi anemia DNA damage response.* Nat Commun, 2019. **10**(1): p. 2849.
35. Kwon, Y., et al., *DNA binding and RAD51 engagement by the BRCA2 C-terminus orchestrate DNA repair and replication fork preservation.* Nat Commun, 2023. **14**(1): p. 432.
36. Parplys, A.C., et al., *NUCKS1 is a novel RAD51AP1 paralog important for homologous recombination and genome stability.* Nucleic Acids Res, 2015. **43**(20): p. 9817-34.
37. Zhao, W., et al., *BRCA1-BARD1 promotes RAD51-mediated homologous DNA pairing.* Nature, 2017. **550**(7676): p. 360-365.

38. Zhao, W., et al., *Promotion of BRCA2-Dependent Homologous Recombination by DSS1 via RPA Targeting and DNA Mimicry.* Mol Cell, 2015. **59**(2): p. 176-87.
39. Wiese, C., et al., *Disparate requirements for the Walker A and B ATPase motifs of human RAD51D in homologous recombination.* Nucleic Acids Res, 2006. **34**(9): p. 2833-43.
40. Dray, E., et al., *Enhancement of RAD51 recombinase activity by the tumor suppressor PALB2.* Nat Struct Mol Biol, 2010. **17**(10): p. 1255-9.
41. Ostvold, A.C., et al., *Molecular cloning of a mammalian nuclear phosphoprotein NUCKS, which serves as a substrate for Cdk1 in vivo.* Eur J Biochem, 2001. **268**(8): p. 2430-40.
42. Sirbu, B.M., F.B. Couch, and D. Cortez, *Monitoring the spatiotemporal dynamics of proteins at replication forks and in assembled chromatin using isolation of proteins on nascent DNA.* Nat Protoc, 2012. **7**(3): p. 594-605.
43. Campeau, E., et al., *A versatile viral system for expression and depletion of proteins in mammalian cells.* PLoS One, 2009. **4**(8): p. e6529.
44. Somyajit, K., et al., *Homology-directed repair protects the replicating genome from metabolic assaults.* Dev Cell, 2021. **56**(4): p. 461-477 e7.
45. Wiese, C., et al., *Promotion of homologous recombination and genomic stability by RAD51AP1 via RAD51 recombinase enhancement.* Mol Cell, 2007. **28**(3): p. 482-90.
46. Modesti, M., et al., *RAD51AP1 is a structure-specific DNA binding protein that stimulates joint molecule formation during RAD51-mediated homologous recombination.* Mol Cell, 2007. **28**(3): p. 468-81.
47. Petermann, E., et al., *Hydroxyurea-stalled replication forks become progressively inactivated and require two different RAD51-mediated pathways for restart and repair.* Mol Cell, 2010. **37**(4): p. 492-502.
48. Thangavel, S., et al., *DNA2 drives processing and restart of reversed replication forks in human cells.* J Cell Biol, 2015. **208**(5): p. 545-62.
49. Vujanovic, M., et al., *Replication Fork Slowing and Reversal upon DNA Damage Require PCNA Polyubiquitination and ZRANB3 DNA Translocase Activity.* Mol Cell, 2017. **67**(5): p. 882-890 e5.
50. Kile, A.C., et al., *HLTF's Ancient HIRAN Domain Binds 3' DNA Ends to Drive Replication Fork Reversal.* Mol Cell, 2015. **58**(6): p. 1090-100.
51. Mazina, O.M., et al., *Polarity and bypass of DNA heterology during branch migration of Holliday junctions by human RAD54, BLM, and RECQ1 proteins.* J Biol Chem, 2012. **287**(15): p. 11820-32.
52. Unk, I., et al., *Role of yeast Rad5 and its human orthologs, HLTF and SHPRH in DNA damage tolerance.* DNA Repair (Amst), 2010. **9**(3): p. 257-67.
53. Fugger, K., et al., *FBH1 Catalyzes Regression of Stalled Replication Forks.* Cell Rep, 2015. **10**(10): p. 1749-1757.
54. Vaitsiankova, A., et al., *PARP inhibition impedes the maturation of nascent DNA strands during DNA replication.* Nat Struct Mol Biol, 2022. **29**(4): p. 329-338.
55. Hanzlikova, H., et al., *The Importance of Poly(ADP-Ribose) Polymerase as a Sensor of Unligated Okazaki Fragments during DNA Replication.* Mol Cell, 2018. **71**(2): p. 319-331 e3.
56. Maya-Mendoza, A., et al., *High speed of fork progression induces DNA replication stress and genomic instability.* Nature, 2018. **559**(7713): p. 279-284.
57. Bryant, H.E., et al., *Specific killing of BRCA2-deficient tumours with inhibitors of poly(ADP-ribose) polymerase.* Nature, 2005. **434**(7035): p. 913-7.
58. Quinet, A., et al., *DNA Fiber Analysis: Mind the Gap!* Methods Enzymol, 2017. **591**: p. 55-82.
59. Tian, T., et al., *The ZATT-TOP2A-PICH Axis Drives Extensive Replication Fork Reversal to Promote Genome Stability.* Mol Cell, 2021. **81**(1): p. 198-211 e6.

60. Joseph, S.A., et al., *Time for remodeling: SNF2-family DNA translocases in replication fork metabolism and human disease.* DNA Repair (Amst), 2020. **95**: p. 102943.
61. Alexeev, A., A. Mazin, and S.C. Kowalczykowski, *Rad54 protein possesses chromatin-remodeling activity stimulated by the Rad51-ssDNA nucleoprotein filament.* Nat Struct Biol, 2003. **10**(3): p. 182-6.
62. Jaskelioff, M., et al., *Rad54p is a chromatin remodeling enzyme required for heteroduplex DNA joint formation with chromatin.* J Biol Chem, 2003. **278**(11): p. 9212-8.
63. Petukhova, G., S. Stratton, and P. Sung, *Catalysis of homologous DNA pairing by yeast Rad51 and Rad54 proteins.* Nature, 1998. **393**(6680): p. 91-4.
64. Ristic, D., et al., *The architecture of the human Rad54-DNA complex provides evidence for protein translocation along DNA.* Proc Natl Acad Sci U S A, 2001. **98**(15): p. 8454-60.
65. Bugreev, D.V., F. Hanaoka, and A.V. Mazin, *Rad54 dissociates homologous recombination intermediates by branch migration.* Nat Struct Mol Biol, 2007. **14**(8): p. 746-53.
66. Bugreev, D.V., O.M. Mazina, and A.V. Mazin, *Rad54 protein promotes branch migration of Holliday junctions.* Nature, 2006. **442**(7102): p. 590-3.
67. Berti, M., D. Cortez, and M. Lopes, *The plasticity of DNA replication forks in response to clinically relevant genotoxic stress.* Nat Rev Mol Cell Biol, 2020. **21**(10): p. 633-651.
68. Berti, M., et al., *Sequential role of RAD51 paralog complexes in replication fork remodeling and restart.* Nat Commun, 2020. **11**(1): p. 3531.
69. Bansbach, C.E., et al., *The annealing helicase SMARCAL1 maintains genome integrity at stalled replication forks.* Genes Dev, 2009. **23**(20): p. 2405-14.